




Stretchable strain sensor facilely fabricated based on multi-wall carbon nanotube composites with excellent performance

Xiang Fu^{1,*} , Maximiano Ramos¹, Ahmed M. Al-Jumaily¹, Ata Meshkinzar¹, and Xiyong Huang¹

¹ Institute of Biomedical Technologies, Auckland University of Technology, Auckland, New Zealand

Received: 4 July 2018

Accepted: 20 September 2018

Published online:

24 September 2018

© Springer Science+Business Media, LLC, part of Springer Nature 2018

ABSTRACT

In recent years, the increasing demand for flexible and wearable devices requires the synthesis of novel stretchable and piezoresistive materials. Piezoresistive polymer composites are popular due to their excellent piezoresistivity and high stretchability, which can readily be attached to clothes or human body. In this study, a stretchable and sensitive strain sensor based on multi-wall carbon nanotube (MWCNT)/polydimethylsiloxane (PDMS) composite with an excellent overall performance was fabricated in a facile and effective way. The composite with 7% MWCNTs is ideal for strain sensor compared to those with 5% and 9% MWCNTs. Not only can the gauge factor reach 5–9 under 10–40% strain, but also the curve of relative change in resistance versus strain is almost linear. The strain sensor can respond immediately with low hysteresis. The strain sensor also exhibits great stability under 1000 cycles of stretching/releasing, demonstrating the desirable long-term endurance to mechanical stimuli as well. The strain sensor was then implemented to monitor human motions (finger and wrist bending), precisely sensing the motion deformation and states. In conclusion, the reported sensor based on MWCNT/PDMS composite possesses numerous favorable characteristics including high sensitivity, good stretchability, ease of fabrication, and promising practical application in the field of biomedical system and wearable electronic devices.

Introduction

Stretchable piezoresistive polymer composites have attracted a great deal of attention due to their excellent endurance for human motion and sensitivity, compared to conventional sensors based on metal

foils or semiconductors [1–3]. Apparently, conventional sensors cannot undergo larger strain ($\gg 5\%$) and present a bad mechanical compliance with human motions. Thus, stretchable polymer composites exhibit enormous potential to be employed for making electronic skins [4, 5], human motion detectors [6, 7], human health monitoring [8, 9], and so

Address correspondence to E-mail: xfu@aut.ac.nz

forth [10, 11]. There are still other advantages of stretchable polymer composites besides high stretchability and good sensitivity, including facile fabrication approach, lightweight, and low cost [12, 13]. The stretchable piezoresistive nanocomposite is mainly fabricated by embedding and dispersing conductive fillers into stretchable polymer matrices. Owing to the percolation network in a matrix constructed by conductive fillers, the composite can keep electromechanical stability with large strain [14]. There are a variety of conductive fillers, such as carbon nanotubes (CNTs) [15, 16], carbon nanofibers [17, 18], graphene [19, 20], and silver nanowires [21], all of which are usually popular with researchers to manufacture strain sensors.

CNTs have unique mechanical and electrical properties in contrast to other conductive fillers. Besides the well-known electrical properties of CNTs, their curvilinear structure and intertwining attribute help to improve the stretchability and piezoresistivity of the composite when CNTs are embedded into the polymer. That is, the curvilinear shapes of CNTs make them more inclined to construct the network in the polymer matrices, which helps to enhance their piezoresistivity [22]. In addition, CNTs are able to withstand relatively higher stretch owing to their mutual intertwinement [23, 24]. For instance, Amjadi et al. [21] reported a strain sensor prepared by silver nanowire–elastomer composite. In spite of the acceptable stability and durability, the sensitivity could not reach the extent of CNTs (the gauge factor (GF) is around 2). In contrast, the sensor that Wang et al. [16] proposed based on CNT/elastomeric trisocyanate-crosslinked polytetrahydrofuran composite, possessed higher gauge factor (up to 90). Nevertheless, some of the properties of CNTs have negative influence on CNT nanocomposites. The agglomeration of CNTs, which is very easy to form in the composite, would adversely affect the mechanical properties and electrical conductivity [25]. On the whole, CNTs seem to be the best candidate compared with other conductive fillers to make piezoresistive materials provided that CNTs could be distributed in the matrix uniformly or homogeneously. Despite the fact that single-wall carbon nanotubes (SWCNTs) possess more outstanding electrical properties in comparison with multi-wall carbon nanotubes (MWCNTs), the expensive price and agglomeration make them not as economic as MWCNTs. Meanwhile, maintaining good compatibility and

interaction of CNTs with polymer matrices significantly affects the piezoresistivity of composites, such as hysteresis and durability [15]. This is mainly related to the fabrication approach and the selection of polymer. Although great progress has been made in the field of CNT composites, it is still a great challenge to prepare the high-performance stretchable strain sensor through a facile approach, ensuring all the fundamental properties of sensors are favorable simultaneously. For instance, Robert et al. [26] invented a sensor made of PC-CNT nanocomposite. Although it exhibited favorable sensitivity (GF up to 100), the hysteresis and stretchability could not be relatively satisfactory. Hence, fabrication of piezoresistive composites with good and balanced fundamental sensing properties is vital for further applications.

Herein, we developed an improved and facile fabrication method to prepare MWCNT/PDMS nanocomposites in order to reduce agglomeration, preparation time and cost. The stretchable sensor is assembled based on the common sandwich-like structure (MWCNT/PDMS nanocomposite which is wrapped in two PDMS layers). The as-prepared strain sensor not only provides adequate stretchability and great sensitivity, but also it possesses instant response time, favorable durability, and low hysteresis. Furthermore, the sensor is employed to detect human motion. When they are mounted on the wrist or finger, they can monitor the motions promptly and accurately. With remarkable overall properties, the CNT/PDMS composite would have a considerable potential to be used as a wearable electronics device in future.

Experiment investigation

Materials

Multi-walled carbon nanotubes (MWCNTs) were purchased from Graphene Supermarket. The diameter of MWCNTs ranges from 50 to 85 nm, and their lengths lie in the range from 10 to 15 μm . The pentane was supplied by Sigma Aldrich, while the PDMS and its curing agent were bought from Dow Corning Company (Sylgard 184).

Fabrication of the MWCNT composite

At first, MWCNTs were poured into the pentane and the mixture solution was dispersed by the horn ultrasonicator for half an hour to disperse MWCNTs. Due to the low boiling point of pentane, we put the mixture solution in cold water to retard the rapid evaporation of the pentane. Meanwhile, the PDMS prepolymer was magnetically stirred in the pentane for 15 min, making it completely dissolved. After that, these two solutions were blended together and continued to be ultrasonicated for 1 h. Next, the curing agent was added to the mixture and stirred moderately. In order to remove the pentane in the mixture, the mixture was heated at 40 °C for evaporation and ultrasonicated simultaneously. Quick evaporation of the pentane not only guarantees little pentane left in the mixture, but also decelerates re-agglomeration of MWCNTs [27]. This provided us with the uniform suspension of MWCNTs and PDMS. Notably, in order to find out the most suitable concentration of MWCNTs for stretchable sensors, we prepared 5%, 7%, and 9% MWCNT/PDMS mixture suspensions, respectively.

Afterward, the mixture was uniformly coated onto a glass plate using a blade and then put into the vacuum oven to degas. This step should be carried out repeatedly until there is almost no bubble on the surface of the mixture membrane as a result of the high viscosity of the mixture which is induced by the intensive network of MWCNTs in the PDMS matrix. It is helpful to make CNTs with better mutual connection. The membrane was sequentially heated at 80 °C for 2 h. Finally, the glass plate with membrane was taken out from the oven, and the final membrane was peeled off from the glass plate. Noticeably, the experimental specific data are listed in Table S1.

Sensors fabrication

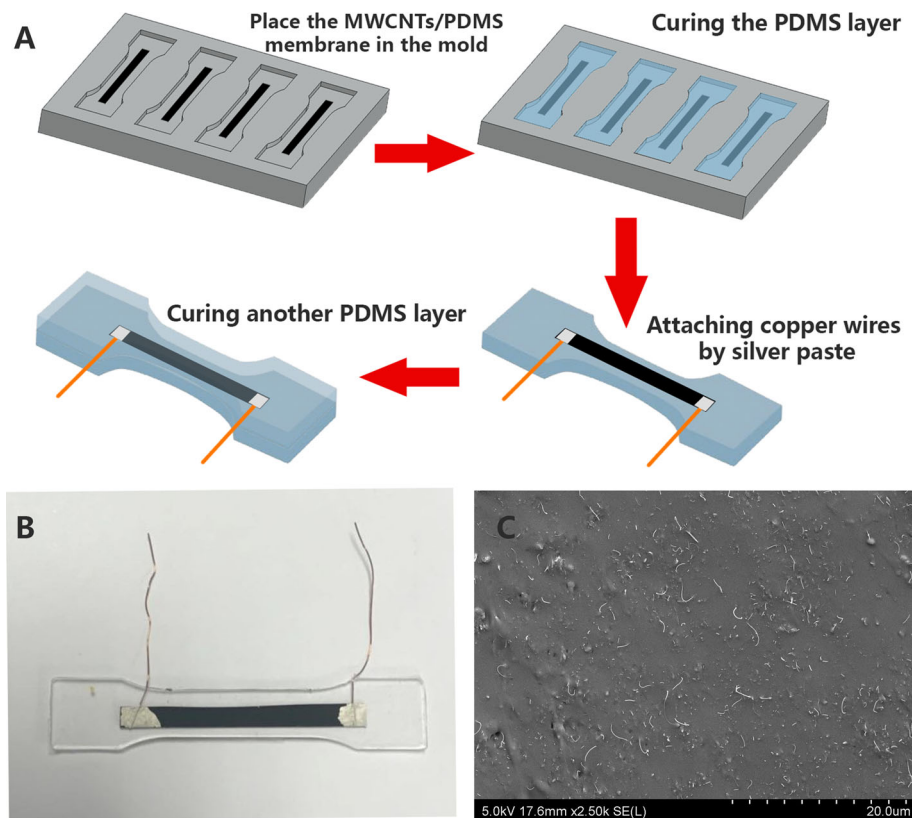
Figure 1a depicts the step-by-step procedure of making the stretchable sensor. The MWCNT/PDMS membrane was cut into some sections with rectangular shapes. After placing them into the alumina mold, the mixture of PDMS prepolymer and curing agent was cast into the mold and covered the membrane. This was followed by curing at 80 °C for 2 h. After that, the PDMS layer adheres to the MWCNT/PDMS layer and then the whole adhered layer was peeled off from the mold due to the penetration of the

liquid PDMS into the composite. Then, two copper wires were attached onto the two ends of the MWCNT/PDMS membrane by silver paste. Finally, another layer of liquid PDMS was cured on the top of the MWCNT/PDMS layer to form a sandwich-like structure as displayed in Fig. 1b. Thus, there are three layers in total. Top and bottom layers are PDMS, while the middle layer is the MWCNT/PDMS composite layer. Notably, due to the penetration of liquid PDMS, the top layer of PDMS can firmly combine with the other two layers. Moreover, the adhesive force between these layers induced by the penetration of PDMS is big enough to guarantee these layers can be stretched together with a large strain [28]. Based on the previous tension test (Supporting Information Figure S1), Young's modulus of the MWCNT/PDMS composite is bigger than that of the pure PDMS. Thus, the adhesive force between these layers will give a shear force to the MWCNT/PDMS layer in order to make it stretched as long as the outer PDMS layer. Once the strain gets beyond a certain value, the adhesive force cannot sustain sufficient shear force to make the composite layer stretched and the composite layer will detach from the outer PDMS layer [28, 29]. Due to the encapsulation of PDMS, the sensor can be directly mounted on the skins without wrinkling and plastic deformation to the middle nanocomposite membrane. The length of conductive section of the sensor (the section between two silver pastes) is around 35 mm. The stretched length and original length are measured as illustrated in Figure S2 (refer to the supporting information).

Sensors characterization

The microstructure of MWCNT/PDMS composite was observed using scanning electron microscope (SEM, Hitachi SU-70). The electrical conductivity and piezoresistivity of sensors were measured using a UNI-T UT803 multimeter by a standard two-probe method. The tension test was conducted using TA.XT plus microforce analyzer to study the hysteresis, durability, sensitivity, and so on. It is worth noting that the clamps of the analyzer should clamp the two ends of the sample and cover the silver paste section to avoid tension of silver paste as shown in Supporting Information Figure S2.

Figure 1 **a** Fabrication procedure of the strain sensor based on MWCNT/PDMS composite with sandwich-like structure. **b** Photographs of the as-prepared sandwich-like strain sensor connected with copper wires. **c** The SEM image of the cross section of the MWCNT/PDMS composite containing 7% MWCNTs.



Results and discussion

Effect of MWCNT concentration on electrical property

At first, the stretchable MWCNT/PDMS composites were manufactured with different concentrations of MWCNTs (5%, 7%, and 9%). Their electrical conductivities expressed by the electrical resistance were compared as shown in Table S2 in supporting information. 5% MWCNT composite membrane exhibits poor and unstable electrical conductivity, electrical resistance ranging from 263.18 to 1028.64 k Ω , whereas the resistance of 7% fluctuates from 4.54 to 20.36 k Ω . 9% MWCNT nanocomposite has the most stable and excellent electrical resistance (0.175–0.341 k Ω). It can also be clearly seen that the standard deviations of electrical resistance for composites with different MWCNT concentrations reduce by increasing the MWCNT concentration. This reveals the unstable resistance of the composites with low MWCNT concentration. The reason is related to the fact that it has less probability to construct conductive network [29, 30]. In the context, without an adequate quantity of CNTs to construct

conductive paths, it is mainly dependent on the network structure. Conversely, once there is a sufficient quantity of CNTs, the network structure will not play an important role. Furthermore, with more additions of CNTs, the electrical conductivity of the composite will not increase as quickly as it did initially. For better observing the dispersion state of the MWCNTs in the PDMS matrix, the corresponding SEM images of cross sections for all samples with 5 K magnification were taken as shown in Figure S3. It can be clearly seen that CNTs are homogeneously dispersed in the matrix for three SEM images of cross sections. The cross-sectional image of the composite with 5% MWCNTs exhibits less MWCNTs (Figure S3a), thus with less connected network, whereas for the composite with 9% MWCNTs (Figure S3c), the cross-sectional image is full of connected network constructed by MWCNTs. This characteristic indirectly reflects the relationship among electrical conductivity, concentration of CNTs and network structure (dispersion state).

The sensitivity of the composite sensors is investigated as depicted in Figure S4. It shows that the relative change in resistance of all the composites with different MWCNT concentrations experiences a rise

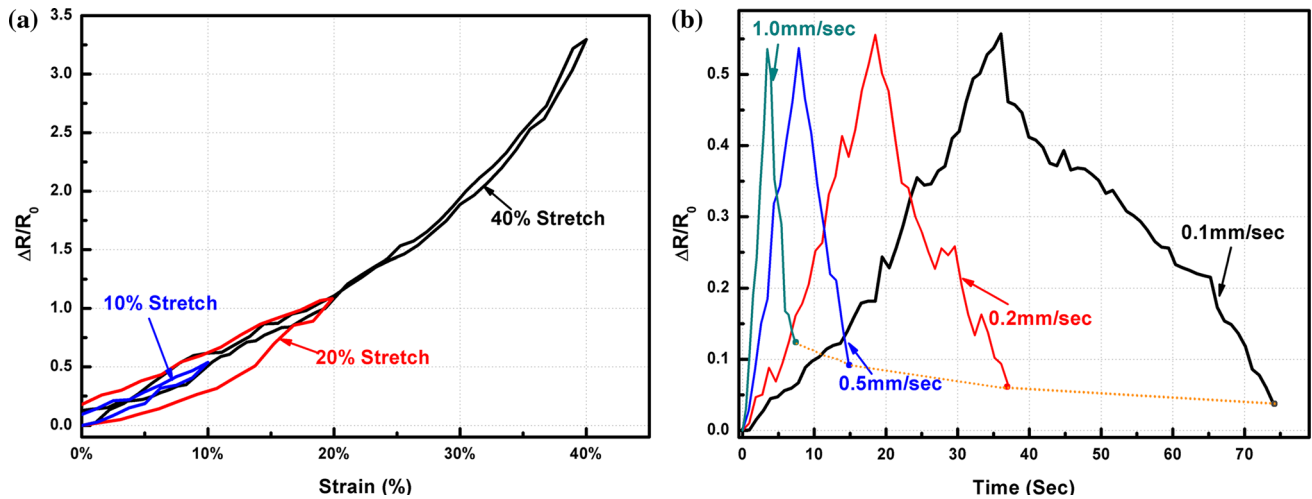


Figure 2 a Curve of relative change in resistance against the applied strain upon stretching in different strain for the sandwich-like sensor. b The correlation between the relative variation in resistance versus time subjected stretching of 10% strain at different tension speeds.

when subjected to stretching, which can be ascribed to the reconstruction of the percolation network. In fact, both the formation and separation can act at the same time over the course of stretching, which might be the reason why the relative change in resistance would increase in an oscillating pattern [31]. Additionally, when adjacent CNTs begin to separate, the tunneling resistance between them will increase which results in an increase in the total resistance [32, 33]. Among the three composites, the one containing 5% MWCNTs has the best gauge factor (GF), approximately equal to 15. The GF is defined as $GF = \frac{\Delta R/R_0}{\varepsilon}$, where ΔR is the change between the current resistance and the initial resistance, R_0 is the initial resistance, and ε denotes the strain in the longitudinal direction. $\Delta R/R_0$ is called relative change in resistance. However, the relationship of relative change in resistance versus strain is not close to linearity and experienced drastic wavelike rise after strain 25%. This is because a large number of the connected paths of CNTs start to break. Although a few of them recombine simultaneously, the effect of breaking is more significant. The composite with 7% MWCNTs has an approximately linear curve of the relative change in resistance against the applied strain (GF ranging from 5 to 9), while the GF of 9% MWCNTs is relatively small ($GF \approx 1$). The denser network constructed by MWCNTs leads to generating more conductive paths, avoiding drastic increases of resistance under stretching. While stretched, the electrical conductivity will not significantly decrease as long as the effective conductive paths are

maintained by sufficient quantity of MWCNTs [34]. Although the sensitivity turns relatively mediocre, the sensor responds to the strain variation with outstanding linearity for the whole process (from 0 to 40%). From above, it can be found that the sensitivity of 9% MWCNT composite sensor is not as high, and the curve of relative change in resistance versus the applied strain for 5% of MWCNTs is not linear enough. Hence, the 7% MWCNT sensor is the most suitable, which relatively has the most stable electrical conductivity, favorable sensitivity, excellent linearity, and good stretchability. In addition, the microstructure of the MWCNT/PDMS is observed by the SEM image to examine the dispersion state of MWCNTs as shown in Fig. 1c. It indicates that MWCNTs are dispersed evenly with little agglomeration so that the existence of conductive network is verified.

Piezoresistivity characterization

The 7% MWCNT sensor undergoes stretching/relaxing cycle with different applied strains, respectively (10%, 20%, and 40%), and the tension speed is set to 0.5 mm/s. The dependence of relative change in resistance and strain history is displayed in Fig. 2a. No matter what the applied strain is, the slopes of the curve of relative change in resistance against the applied strain are close, which indicates that the sensor has excellent stability and linear response to mechanical stimuli. That is to say, the gauge factor of the sensor ranges from 5 to 9 upon stretching within

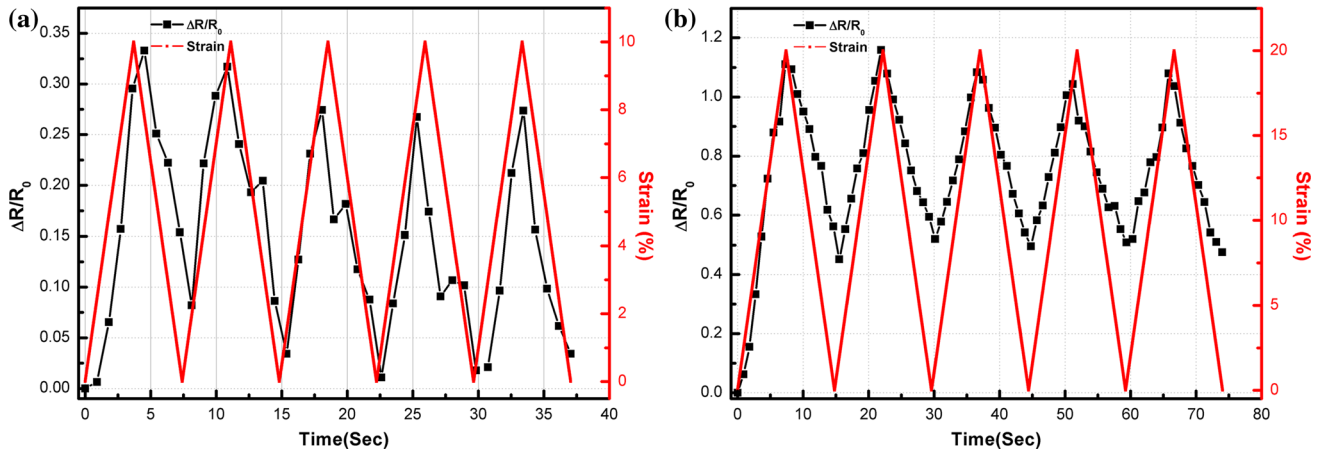


Figure 3 Resistance response of the strain sensor to the cycle of stretching/releasing with 0–0% strain variation (a) and 0–20% strain variation (b).

strain 40%. The CNT-based sensor made by Wang et al. possessed unstable gauge factor, which varied from 10 to 50 under strain 40% [16]. Besides, the graphene-based strain sensor fabricated by Park et al. only exhibited gauge factor of around 1. Hence, this sensor has excellent sensitivity [20]. Furthermore, the relative change in resistance diminishes promptly when the sensor starts to be released. The trace of relative resistance variation curve is very close for both cases of stretching and releasing cycles. In other words, the hysteresis performance of the sensor is good. The hysteresis of electrical resistance might be slightly affected by the slippage of CNTs upon stretching [13]. Besides, the hysteresis of PDMS perhaps contributes to the sensor hysteresis to some extent [35]. To better understand the hysteresis performance, the hysteresis error is introduced here. Based on the hysteresis error equation,

$$\gamma_H = \frac{\Delta H_{max}}{Y} \times 100\% \tag{1}$$

where the γ_H is the hysteresis error index, while ΔH_{max} is the maximum difference between the $\Delta R/R_0$ in stretching and releasing cycles, and Y denotes the maximum full-scale $\Delta R/R_0$, respectively. The hysteresis error index for 20% strain is 30.4%, whereas that for 10% strain is 16.8% and for 40% strain is 9.3%. Although the hysteresis for 20% strain is larger than the other two, the error still can be tolerable. For example, the carbon black/PDMS composite sensor fabricated by Kong et al. [36] exhibited hysteresis error around 25% upon stretching of 10% strain.

Amjadi et al. [21] made a stretchable sensor composed of silver nanowire–elastomer nanocomposite which presented hysteresis error roughly 30% subjected to 10% strain stretching. It is perhaps attributed to the fact that the network of CNTs would reconfigure differently in each stretching. Therefore, the hysteresis error only can be guaranteed to be under an acceptable limit.

Considering that the tension speed is one of the main influential parameters on the piezoresistivity performance, herein the piezoresistive behavior of the sensor is studied at different tension speeds. The sensor is stretched up to 10% strain at different tensile speeds as illustrated in Fig. 2b. It can be seen that not only the sensitivity remains stable, but also the curve of relative resistance change versus time maintains its linearity. In other words, the strain gauge exhibits a strain-rate-independent piezoresistive response in terms of sensitivity and linearity. However, the response time is slightly different when subject to stretching/releasing with different tensile speeds. As shown in Figure S5, when the tension speed is 0.5 mm/s and 1 mm/s, the electrical resistance response will produce a slight delay, which could be observed through comparing the peaks of $\Delta R/R_0$ –time curve and strain–time curve. Nevertheless, when the sample was stretched at a rate of 0.1 mm/s or 0.2 mm/s, the delay can be neglected. It might be attributed to the error caused by the resolution limit of the multimeter, or it is probably induced by the hysteresis of the PDMS [35, 37]. Furthermore, quicker

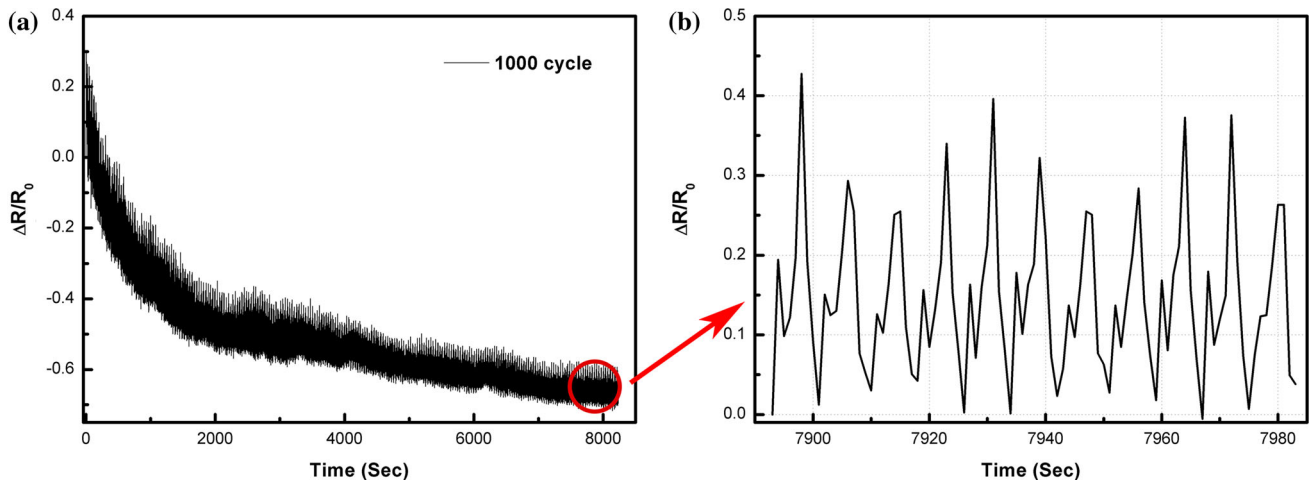


Figure 4 **a** Long-term relative variation in resistance of the strain sensor when subjected to the 1000 cycles of stretching/releasing (from 0–10% strain). **b** The relative change in resistance of the strain sensor magnified from the red circle part in (a).

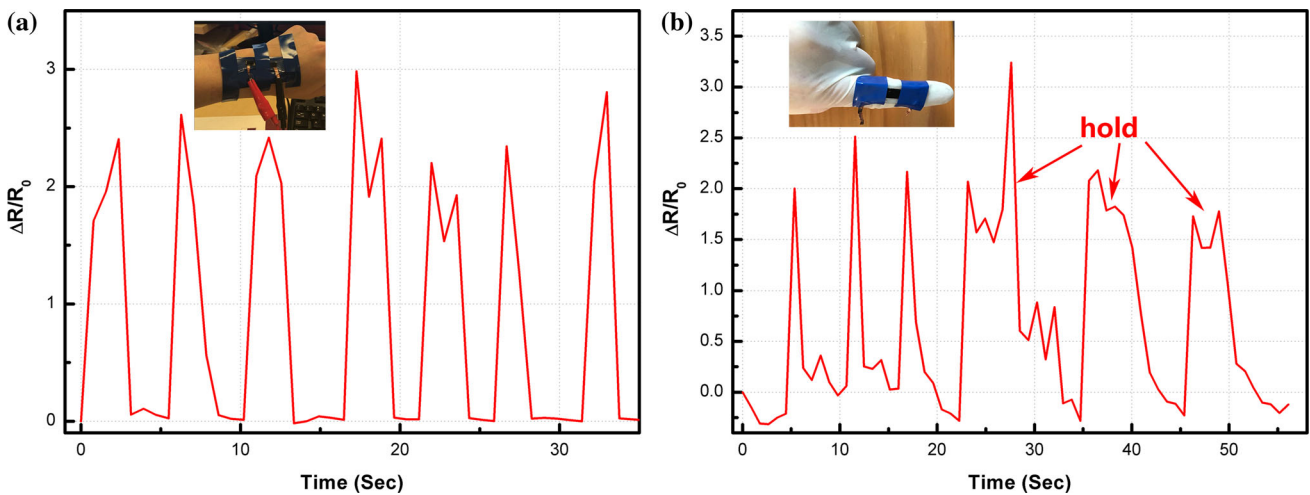


Figure 5 **a** Curve of relative change in resistance versus time for the strain sensor when subjected to wrist bending. **b** The dependence of relative change in resistance and time of the strain sensor under finger bending with two motion states.

tensile speed would lead to a bigger difference between initial and ending resistance, which can be explained by the fact that the CNTs cannot go back to the balanced state promptly in the PDMS matrix due to the presence of friction between the CNTs and PDMS [38, 39]. That is to say, quick tensile speed does not offer sufficient time to make internal structure reaching balanced and stable status. To be specific, as the sensor is stretched the MWCNT network structure reshapes at the same time, so the neighboring MWCNTs need time to reach the equilibrium state mutually again through the van der Waals interactions between them and the interactions between CNTs and PDMS [40–42].

Figure 3a exhibits the dynamic relative resistance change response of the sensor incorporating 7% MWCNTs to the strain variation (0–10%) under stretching/relaxing cycles at a tension rate of 1 mm/s. As indicated in the figure, the profile of the change in resistance has greatly overlapped the strain profile, manifesting that the sensor has prompt response speed. Although the resistance after the cycle of stretching/releasing cannot go back to the initial value at once, the difference is tiny enough to neglect. In addition, the GF still reaches around 2. In contrast, the sensor is also applied on stretching and releasing with 0–20% strain at the same tension speed as illustrated in Fig. 3b. As expected, the profile of the

relative change in resistance almost precisely followed the strain variation, in spite of one remarkable phenomenon that the resistance after the first cycle of stretching/releasing cannot go back to the initial value. However, in the following cycles, not only does the value of the relative change in resistance in each valley vary marginally less than 1%, but also its curve against time shows stable wave variation. This phenomenon is mainly caused by the frictions between the CNTs and PDMS [38]. Due to the high tension strain and CNTs slippage, CNT percolation network in the PDMS matrix upon releasing is unable to recover to the stable and balanced structure fully and promptly. Hence after the first cycle, the values of relative change in resistance in the valleys are bigger than the initial value and then stay similar. Besides, in the 10% strain stretching/releasing cycle, the resistance after every cycle can recover to the initial value approximately because the relatively small strain does not lead to the delay time of recovery. In any case, when the sensor is subjected to sequential stretching/relaxing cycles with 10 or 20% strain, it still shows a desirable consistency between resistance change and strain variation.

The durability which is an important indicator for the strain sensor represents the endurance to the long-term stretching/releasing cycles with excellent mechanical and electrical performance simultaneously. As depicted in Fig. 4a, the strain sensor was stretched and relaxed circularly 1000 times with 10% strain at the tension speed of 1 mm/s. The bulk electrical resistance of the sensor experiences a quick drop at the initial phase, and then it slightly diminishes. To the best of our knowledge, two competitive processes that are destruction and formation of conductive paths work during the stretching of composites [42]. In the region where CNTs are dispersed evenly, the conductive paths would be destroyed remarkably under stretching process. Due to the sufficient aggregation of MWCNTs in the region of CNT clusters, conductive channels of CNTs would not be destructed. Instead, the clusters of MWCNTs may be separated apart gradually when the sensor is repeatedly stretched and released, resulting in the formation of more conductive paths in the MWCNT agglomeration regions [43, 44]. This demonstrates that the initial resistance after each cycle decreases. Moreover, with the progressive separation of CNT agglomeration, the downtrend of resistance slows down and the resistance will approach one

stable value. Besides, the CNTs would become aligned in stretching direction after a series of stretching/releasing [45]. As a consequence, this may help to improve the electrical conductivity along the stretching direction, but the sensitivity may be deteriorated [46, 47]. Furthermore, after a large number of stretching/releasing, the sensor still exhibits the stable sensitivity and quick response time when subjected to strain variation, which can be seen in the detailed view of the red circle part (Fig. 4b).

After a series of characterization, the sensor proves that it has a desirable overall performance. It not only exhibits favorable sensitivity, low hysteresis, and quick response, but also it can adapt to different tension speeds and guarantee the sufficient longevity. In the end, the as-prepared strain sensor was employed for detection of human motions to observe whether it can be eligible for these tasks or not.

The deformation of the majority of human motions, such as wrist and finger bending, typically would not give rise to strain exceeding 40% [48]. Figure 5a shows the relative change in resistance when subjected to wrist bending. This process was recorded (see in Supporting Information Movie 1). After a set of bending cycles, the relative change in resistance exhibits stable and similar waveforms, demonstrating a desirable reproducibility of the sensor. Furthermore, the maximum values of relative variation in resistance lie in the range from 2 to 2.5. In contrast to Fig. 2a, it is evident that the deformation of wrist bending is around 30–35% as presented elsewhere in the literature [48, 49]. Besides, the finger bending was detected by two different motions, like quick bending/relaxing and bending/holding/relaxing, as shown in Supporting Information Movie 2. The relative change in resistance leveled on one value while the finger maintained the bending state until the finger was unbent. This phenomenon provided evidence that the sensor possesses high sensitivity and prompt response speed.

Conclusion

In summary, the stretchable MWCNT/PDMS composite was manufactured through a facile and effective approach and then encapsulated by PDMS with sandwich-like structure. After comparison and analysis, the composite containing 7% MWCNTs is the most suitable for making the stretchable sensor. Also, it can be seen that MWCNTs is dispersed fairly uniformly in the

PDMS matrix by observing SEM images. The as-prepared strain sensor not only exhibits high stretchability which was able to be stretched as high as 40% of its original length, but also it shows high sensitivity ranging from 3 to 5. In addition, the sensor can respond immediately and precisely when subjected to a succession of stretching/releasing cycles with low hysteresis. Furthermore, the strain sensor still performs well after 1000 stretching/releasing cycles, demonstrating favorable durability. In the end, the practical employment of the strain is verified by the fact that the sensors can detect wrist bending precisely and promptly as well as the discrimination between two finger bending motions. Considering these advantages of the strain sensor, it is trustworthy that both the sensor and the composite have potentials to be utilized in various fields, including wearable devices, biomedical detectors.

Acknowledgements

This work was supported by the Institute of Biomedical Technologies. We would like to acknowledge Brett Holden and Jim Crossen for their assistance in electrical measurements, and Mark Masterton for mechanical measurements.

Electronic supplementary material: The online version of this article (<https://doi.org/10.1007/s10853-018-2954-4>) contains supplementary material, which is available to authorized users.

References

- [1] Tadakaluru S, Thongsuwan W, Singjai P (2014) Stretchable and flexible high-strain sensors made using carbon nanotubes and graphite films on natural rubber. *Sensors* 14:868–876
- [2] Yao S, Zhu Y (2015) Nanomaterial-enabled stretchable conductors: strategies, materials and devices. *Adv Mater* 27:1480–1511
- [3] Lu N, Lu C, Yang S et al (2012) Highly sensitive skin-mountable strain gauges based entirely on elastomers. *Adv Funct Mater* 22:4044–4050
- [4] Zhao X, Hua Q, Yu R et al (2015) Flexible, stretchable and wearable multifunctional sensor array as artificial electronic skin for static and dynamic strain mapping. *Adv Electron Mater* 1:1500142
- [5] Pang C, Koo JH, Nguyen A et al (2015) Highly skin-conformal microhairy sensor for pulse signal amplification. *Adv Mater* 27:634–640
- [6] Yao S, Zhu Y (2014) Wearable multifunctional sensors using printed stretchable conductors made of silver nanowires. *Nanoscale* 6:2345–2352
- [7] Hwang B-U, Lee J-H, Trung TQ et al (2015) Transparent stretchable self-powered patchable sensor platform with ultrasensitive recognition of human activities. *ACS Nano* 9:8801–8810
- [8] Gong S, Schwab W, Wang Y et al (2014) A wearable and highly sensitive pressure sensor with ultrathin gold nanowires. *Nat Commun* 5:3132
- [9] Wang X, Gu Y, Xiong Z et al (2014) Silk-molded flexible, ultrasensitive, and highly stable electronic skin for monitoring human physiological signals. *Adv Mater* 26:1336–1342
- [10] Li X, Lin Z-H, Cheng G et al (2014) 3D fiber-based hybrid nanogenerator for energy harvesting and as a self-powered pressure sensor. *ACS Nano* 8:10674–10681
- [11] Niu Z, Dong H, Zhu B et al (2013) Highly stretchable, integrated supercapacitors based on single-walled carbon nanotube films with continuous reticulate architecture. *Adv Mater* 25:1058–1064
- [12] Amjadi M, Yoon YJ, Park I (2015) Ultra-stretchable and skin-mountable strain sensors using carbon nanotubes—ecoflex nanocomposites. *Nanotechnology* 26:375501
- [13] Fan Q, Qin Z, Gao S et al (2012) The use of a carbon nanotube layer on a polyurethane multifilament substrate for monitoring strains as large as 400%. *Carbon* 50:4085–4092
- [14] Lee P, Lee J, Lee H et al (2012) Highly stretchable and highly conductive metal electrode by very long metal nanowire percolation network. *Adv Mater* 24:3326–3332
- [15] Yamada T, Hayamizu Y, Yamamoto Y et al (2011) A stretchable carbon nanotube strain sensor for human-motion detection. *Nat Nanotechnol* 6:296–301
- [16] Wang Y, Mi H, Zheng Q et al (2016) Highly stretchable and sensitive piezoresistive carbon nanotube/elastomeric triisocyanate-crosslinked polytetrahydrofuran nanocomposites. *J Mater Chem C* 4:460–467
- [17] Dong Y, Ni Q-Q, Li L et al (2014) Novel vapor-grown carbon nanofiber/epoxy shape memory nanocomposites prepared via latex technology. *Mater Lett* 132:206–209
- [18] Dong Y, Xia H, Zhu Y et al (2015) Effect of epoxy-graft-polyoxyethylene octyl phenyl ether on preparation, mechanical properties and triple-shape memory effect of carbon nanotube/water-borne epoxy nanocomposites. *Compos Sci Technol* 120:17–25

- [19] Tian H, Shu Y, Cui Y-L et al (2014) Scalable fabrication of high-performance and flexible graphene strain sensors. *Nanoscale* 6:699–705
- [20] Park JJ, Hyun WJ, Mun SC et al (2015) Highly stretchable and wearable graphene strain sensors with controllable sensitivity for human motion monitoring. *ACS Appl Mater Interfaces* 7:6317–6324
- [21] Amjadi M, Pichitpajongkit A, Lee S et al (2014) Highly stretchable and sensitive strain sensor based on silver nanowire–elastomer nanocomposite. *ACS Nano* 8:5154–5163
- [22] Cai L, Song L, Luan P et al (2013) Super-stretchable, transparent carbon nanotube-based capacitive strain sensors for human motion detection. *Sci Rep* 3:3048
- [23] Li J, Ma W, Song L et al (2011) Superfast-response and ultrahigh-power-density electromechanical actuators based on hierarchical carbon nanotube electrodes and chitosan. *Nano Lett* 11:4636–4641
- [24] Ma W, Liu L, Zhang Z et al (2009) High-strength composite fibers: realizing true potential of carbon nanotubes in polymer matrix through continuous reticulate architecture and molecular level couplings. *Nano Lett* 9:2855–2861
- [25] Huang Y, Ahir S, Terentjev E (2006) Dispersion rheology of carbon nanotubes in a polymer matrix. *Phys Rev B* 73:125422
- [26] Robert C, Feller JFO, Castro ML (2012) Sensing skin for strain monitoring made of PC–CNT conductive polymer nanocomposite sprayed layer by layer. *ACS Appl Mater Interfaces* 4:3508–3516
- [27] Xue C, Du G-Q, Chen L-J et al (2014) A carbon nanotube filled polydimethylsiloxane hybrid membrane for enhanced butanol recovery. *Sci Rep* 4:5925
- [28] Park M, Kim H, Youngblood JP (2008) Strain-dependent electrical resistance of multi-walled carbon nanotube/polymer composite films. *Nanotechnology* 19:055705
- [29] Wang Z, Ye X (2013) A numerical investigation on piezoresistive behaviour of carbon nanotube/polymer composites: mechanism and optimizing principle. *Nanotechnology* 24:265704
- [30] Panozzo F, Zappalorto M, Quaresimin M (2017) Analytical model for the prediction of the piezoresistive behavior of CNT modified polymers. *Compos B* 109:53–63
- [31] Del Castillo-Castro T, Castillo-Ortega M, Encinas J et al (2012) Piezo-resistance effect in composite based on cross-linked polydimethylsiloxane and polyaniline: potential pressure sensor application. *J Mater Sci* 47:1794–1802. <https://doi.org/10.1007/s10853-011-5965-y>
- [32] Ferreira A, Martínez MT, Ansón-Casaos A et al (2013) Relationship between electromechanical response and percolation threshold in carbon nanotube/poly(vinylidene fluoride) composites. *Carbon* 61:568–576
- [33] Jandro LA, César YK, Gilles PT et al (2015) Strain gauge sensors comprised of carbon nanotube yarn: parametric numerical analysis of their piezoresistive response. *Smart Mater Struct* 24:075018
- [34] Georgousis G, Pandis C, Kalamiotis A et al (2015) Strain sensing in polymer/carbon nanotube composites by electrical resistance measurement. *Compos B* 68:162–169
- [35] Kim TK, Kim JK, Jeong OC (2011) Measurement of non-linear mechanical properties of PDMS elastomer. *Microelectron Eng* 88:1982–1985
- [36] Kong J-H, Jang N-S, Kim S-H et al (2014) Simple and rapid micropatterning of conductive carbon composites and its application to elastic strain sensors. *Carbon* 77:199–207
- [37] Michelis F, Bodelot L, Bonnassieux Y et al (2015) Highly reproducible, hysteresis-free, flexible strain sensors by inkjet printing of carbon nanotubes. *Carbon* 95:1020–1026
- [38] Qin Q, Zhu Y (2011) Static friction between silicon nanowires and elastomeric substrates. *ACS Nano* 5:7404–7410
- [39] Suhr J, Koratkar N, Koblinski P et al (2005) Viscoelasticity in carbon nanotube composites. *Nat Mater* 4:134–137
- [40] Yu X-G, Li Y-Q, Zhu W-B et al (2017) A wearable strain sensor based on a carbonized nano-sponge/silicone composite for human motion detection. *Nanoscale* 9:6680–6685
- [41] Zhanov AI, Pogorelov EG, Chang Y-C (2010) Van der Waals interaction between two crossed carbon nanotubes. *ACS Nano* 4:5937–5945
- [42] Leyva Egorola S, Del Castillo Castro T, Castillo Ortega MM et al (2017) Electrical, mechanical, and piezoresistive properties of carbon nanotube–polyaniline hybrid filled polydimethylsiloxane composites. *J Appl Polym Sci* 134:44780
- [43] Roh E, Hwang B-U, Kim D et al (2015) Stretchable, transparent, ultrasensitive, and patchable strain sensor for human-machine interfaces comprising a nanohybrid of carbon nanotubes and conductive elastomers. *ACS Nano* 9:6252–6261
- [44] Liu C-X, Choi J-W (2014) Analyzing resistance response of embedded PDMS and carbon nanotubes composite under tensile strain. *Microelectron Eng* 117:1–7
- [45] Jin L, Bower C, Zhou O (1998) Alignment of carbon nanotubes in a polymer matrix by mechanical stretching. *Appl Phys Lett* 73:1197–1199
- [46] Hu N, Karube Y, Arai M et al (2010) Investigation on sensitivity of a polymer/carbon nanotube composite strain sensor. *Carbon* 48:680–687
- [47] Park C, Wilkinson J, Banda S et al (2006) Aligned single-wall carbon nanotube polymer composites using an electric field. *J Polym Sci Part B Polym Phys* 44:1751–1762

- [48] Tang Y, Zhao Z, Hu H et al (2015) Highly stretchable and ultrasensitive strain sensor based on reduced graphene oxide microtubes-elastomer composite. *ACS Appl Mater Interfaces* 7:27432–27439
- [49] Wang Y, Wang L, Yang T et al (2014) Wearable and highly sensitive graphene strain sensors for human motion monitoring. *Adv Funct Mater* 24:4666–4670